

# Generalization of atomic random-phase-approximation method for diatomic molecules.

## II. N<sub>2</sub> K-shell photoionization

S. K. Semenov and N. A. Cherepkov

*State University of Aerospace Instrumentation, 190000 St. Petersburg, Russia*

(Received 29 March 2002; published 15 August 2002)

Partial and total photoionization cross sections of the  $K$  shell of the N<sub>2</sub> molecule are calculated using the generalization of the random-phase approximation that has been applied earlier to the valence shells of N<sub>2</sub> [Phys. Rev. A **61**, 032704 (2000)]. At zero order the relaxed core Hartree-Fock approximation is used. It is demonstrated that due to strong intershell correlations the  $\sigma^*$  shape resonance reveals itself not only in the  $1\sigma_g \rightarrow \epsilon\sigma_u$  channel as it takes place in all single-particle approximations, but also in the  $1\sigma_u \rightarrow \epsilon\sigma_g$  channel. The influence of vibrational motion on the cross sections is taken into account. Good agreement with the most recent experimental data for different partial cross sections is achieved.

DOI: 10.1103/PhysRevA.66.022708

PACS number(s): 33.80.Eh

### I. INTRODUCTION

Investigations of photoionization of simple diatomic molecules such as N<sub>2</sub> have a long history, and with application of more sophisticated theoretical methods the agreement between theory and experiment has been steadily improved. Recently, rather good results for the valence shells of N<sub>2</sub> have been demonstrated in Refs. [1–4] by applying the random-phase approximation (RPA). But up to now this method has not been employed for the  $K$  shell of N<sub>2</sub>. In this paper we report on the calculations of partial photoionization cross sections for the  $K$  shells of the N<sub>2</sub> molecule performed using the recently developed version of RPA [1,5]. In Ref. [5] this method has been successfully applied to the calculations of H<sub>2</sub> photoionization cross section, while in Ref. [1] all valence shells of N<sub>2</sub> have been studied. This paper is a direct continuation of the research started in Ref. [1]. The preliminary results of this study supported by experimental measurements have been published earlier in Ref. [6].

Contrary to the atomic case where the role of many-electron correlations in photoionization of the  $K$  shells is rather negligible, in homonuclear diatomic molecules the situation is strongly different due to the presence of two closely spaced  $K$  shells. Many-electron correlations between these two shells appear to be important, changing the magnitudes of some transitions by a factor of 2 [6]. Therefore the application of RPA method to the  $K$  shell of the N<sub>2</sub> molecule is well justified. A number of earlier calculations for the  $K$  shells were performed using various methods, in particular, multiple-scattering method [7,8], the Stieltjes-Tchebycheff moment theory [9], the relaxed core Hartree-Fock (HF) approximation [10], the local-density approximation with the transition state potential [11], and the multichannel Schwinger configuration interaction method [12]. In Refs. [11,12] a good agreement with experiment has been achieved.

The majority of molecular calculations are performed in a fixed-nuclei approximation at the equilibrium geometry. But it was shown rather long ago that the position and strength of the shape resonance are very sensitive functions of the nuclear separation [13,14]. In other words, the nuclear mo-

tion in the ground state is influencing the photoionization process, especially in the vicinity of the shape resonance. To take it into account, it was proposed in Refs. [13,14] to perform calculations for several fixed internuclear separations  $R$  and then to average the photoionization parameters over  $R$  with the vibrational wave function of the initial state. This procedure implies the summation over all (unresolved) vibrational final states. At that time the difference between theory and experiment for the cross sections was frequently about a factor of 2 or even larger, and the role of vibrational averaging was not so important. As a result, in the later investigations this averaging was not performed. Now, getting much closer agreement with the experiment, we need to take into consideration the influence of the vibrational motion, since its contribution is comparable with the difference between theory and experiment. For this goal we performed calculations for several internuclear separations, and then averaged the photoionization parameters with the initial-state vibrational wave function. The results of our calculations are compared with the variety of the newest experimental data, and possible reasons for some discrepancies are discussed.

### II. RPA METHOD

In our calculations a modification of the RPA method is used that was developed earlier for atomic calculations in Ref. [15]. A detailed description of this method was given in Refs. [1,5], therefore here we only briefly outline the main steps. The calculations proceed as following. At first the HF ground-state wave functions are calculated in the fixed-nuclei approximation. With their help the zero-order basis set of single-particle HF wave functions of discrete excited states and of the continuous spectrum is calculated in the field of a frozen core of a singly charged ion (the one-particle–one-hole excited states). With this basis the dipole and the Coulomb matrix elements are calculated. As the next step we are looking for the dipole matrix elements in RPA by solving the corresponding RPA equation, without calculating explicitly the wave functions in RPA. The dipole matrix elements obtained as a solution of the RPA equation are used for a standard calculation of photoionization cross section (see Eq. (5) of Ref. [1]).

The calculations are performed using a partial-wave expansion in prolate spheroidal coordinates as it was frequently used earlier for the bound-state wave functions of diatomic molecules [16–18]. As compared to usual expansion in spherical coordinates, this method substantially reduces the number of terms necessary to take into account in order to reach high accuracy in calculations. Earlier [10] it was shown that a relaxation of the ionic core plays an important role in the photoionization of  $K$  shells of  $N_2$  changing the position and magnitude of the  $\sigma^*$  shape resonance. In particular, in the case of a frozen-core (unrelaxed) HF calculation the maximum appears 5 eV above threshold and has the magnitude two times larger than the experimental one [10]. In the relaxed core HF (RCHF) calculation the maximum is 13 eV above threshold and its magnitude is slightly lower than the experimental one, while the experimental position of maximum is 9 eV above threshold.

Since the core relaxation effects are not taken into account in the RPA method itself, one can take them into account by performing the RPA calculations with the basis set of the RCHF photoelectron wave functions. The latter is found in the following way. At first the self-consistent HF molecular ion wave functions are calculated with the hole in an appropriate shell, either  $1\sigma_g$  or  $1\sigma_u$ , then a set of photoelectron wave functions in the frozen field of the corresponding molecular ion state is found. With these wave functions the dipole and Coulomb matrix elements are calculated entering the RPA equation. The justification for such a procedure was given in Ref. [19] for the case of atomic calculations, and it is equally applied to the molecular case. We performed our first RPA calculations with both HF and RCHF basis sets. The results are qualitatively similar and differ mainly by the position and magnitude of the  $\sigma^*$  shape resonance as was mentioned above. Since with the RCHF basis set a larger part of many-electron correlations is taken into account, we shall present in the following only the results obtained in the RCHF.

As it was shown some time ago [13,14], the vibrational motion changes the cross section obtained in a fixed-nuclei approximation. To take into account the nuclear motion in the initial state, the RPA calculations are at first performed for several internuclear distances  $R$  in a fixed-nuclei approximation. For a given photon energy  $\omega$  the partial photoionization cross sections  $\sigma(\omega, R)$  are calculated separately for every value of  $R$ . After that the vibrational averaged cross sections  $\sigma_{av}(\omega)$  are calculated from the equation,

$$\sigma_{av}(\omega) = \int \chi_i^2(R) \sigma(\omega, R) dR, \quad (1)$$

where  $\chi_i(R)$  is the initial-state vibrational wave function. We assume in this paper that only the ground vibrational state is initially populated.

### III. RESULTS OF CALCULATIONS

Consider at first the results for partial photoionization cross sections. As it was expected, the RPA photoionization cross sections in the length and velocity forms nearly coin-

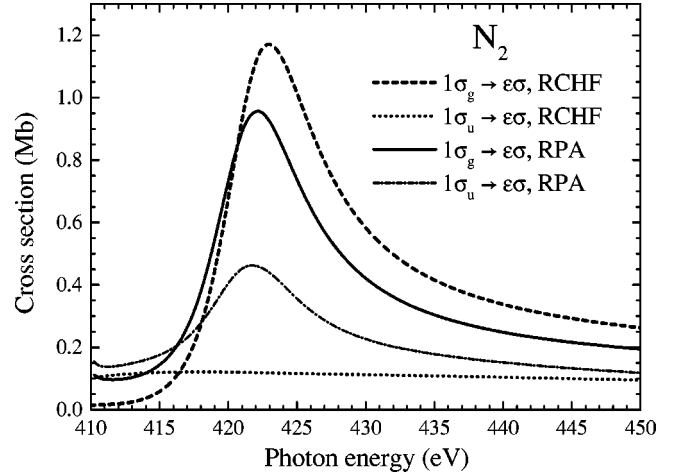


FIG. 1. Photoionization cross sections for the  $K$  shells of the  $N_2$  molecule corresponding to the  $1\sigma_g \rightarrow \epsilon\sigma_u$  and  $1\sigma_u \rightarrow \epsilon\sigma_g$  channels calculated in the RCHF and RPA approximations in the length form.

cide (the difference is usually of the order of 2–3%), but they do not differ much even in the RCHF approximation. Namely, the RCHF cross section in the length form is about 5% higher than in the velocity form. Therefore in the following only the results obtained with the length form of the dipole operator are shown in the figures. The experimental thresholds are used in our calculations.

It is well known from the atomic calculations [15] that the intershell many-electron correlations play a very important role when the ionization thresholds of interacting (sub)shells are close to each other, and when the photoionization cross section of one of them is much larger than that of the other one. On the other hand, it was also well known that the role of many-electron correlations in photoionization of atomic core levels is rather negligible.

In photoionization of the  $K$  shells of homonuclear diatomic molecules the situation is strongly different from the atomic case because there are two closely spaced  $K$  shells. In addition, the photoionization cross section of one shell (the  $1\sigma_g \rightarrow \epsilon\sigma_u$  channels where the  $\sigma^*$  shape resonance occurs) in the RCHF approximation is one order of magnitude larger than the cross section for the other shell (the  $1\sigma_u \rightarrow \epsilon\sigma_g$  channels). It is illustrated in Fig. 1 where we present the photoionization cross sections for the  $1\sigma_g \rightarrow \epsilon\sigma_u$  and  $1\sigma_u \rightarrow \epsilon\sigma_g$  channels calculated in the RCHF approximation. In accord with the calculations of Dehmer and Dill [7,8] the cross section for the  $1\sigma_g \rightarrow \epsilon\sigma_u$  channels in the RCHF approximation has a strong maximum, while for the  $1\sigma_u \rightarrow \epsilon\sigma_g$  channels it is nearly constant in a broad energy range. So, both conditions for many-electron correlations to be important are fulfilled, and therefore strong intershell correlations between the  $1\sigma_g \rightarrow \epsilon\sigma_u$  and  $1\sigma_u \rightarrow \epsilon\sigma_g$  channels are expected. Figure 2 shows the corresponding Feynman diagrams of the lowest order in the Coulomb interaction that give the main contribution in the RPA approximation.

The  $1\sigma \rightarrow \epsilon\sigma$  channels do not interact with the  $1\sigma \rightarrow \epsilon\pi$  ones since the internal forces in a closed system (the Coulomb interaction between electrons in our case) could not change the projection of the total angular momentum. The

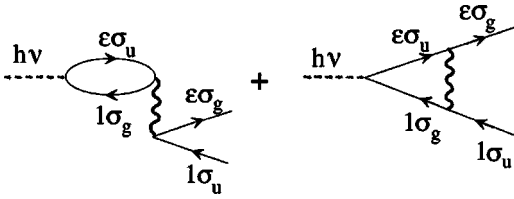


FIG. 2. The lowest-order Feynman diagrams corresponding to the RPA intershell correlations between the  $1\sigma_g \rightarrow \epsilon\sigma_u$  and  $1\sigma_u \rightarrow \epsilon\sigma_g$  channels. Dashed lines describe the photon, wavy lines correspond to the Coulomb interaction, and solid lines with arrows are the particle or hole states.

interaction with the valence shells can be neglected due to a large difference between the ionization thresholds. Therefore we are taking into account the many-electron correlations only between the  $1\sigma_g \rightarrow \epsilon\sigma_u$  and  $1\sigma_u \rightarrow \epsilon\sigma_g$  channels (and separately between the  $1\sigma_g \rightarrow \epsilon\pi_u$  and  $1\sigma_u \rightarrow \epsilon\pi_g$  channels). The cross sections calculated in the RPA are also shown in Fig. 1. Due to the many-electron correlations the pronounced maximum appears in the  $1\sigma_u \rightarrow \epsilon\sigma_g$  cross section, while the maximum in the main  $1\sigma_g \rightarrow \epsilon\sigma_u$  cross section becomes lower. In other words, part of the intensity of the  $\sigma^*$  shape resonance is transferred to the  $1\sigma_u \rightarrow \epsilon\sigma_g$  channels. At the same time, the maximum of the shape resonance in the RPA approximation is shifted by about 1 eV to lower energies, which improves the agreement with the experiment (see below).

We calculated also the contributions of different partial waves to the cross sections. Figure 3 shows our RPA results for the  $1\sigma_g$  shell. In accord with the earlier conclusion made in Refs. [7,8], the main contribution to the  $\sigma^*$  shape resonance is given by the  $f\sigma$  partial wave. It is interesting to mention that very close to the maximum of the shape resonance there is a Cooper minimum in the  $p\sigma$  partial cross section (it exists also in the RCHF approximation at 418-eV photon energy), while the  $h\sigma$  cross section is negligibly small at all energies. Due to that, the  $\sigma^*$  shape resonance is formed practically by a single  $f\sigma$  partial wave, which is most probably an exceptional case. For example, near the shape resonance in the  $2\sigma_g$  shell of  $N_2$  (also formed basically by the  $f\sigma$  partial wave) there is no Cooper minimum in the  $p\sigma$  partial cross section [20]. To prove that there is the shape resonance in the  $f\sigma$  partial wave, it should be shown also that the corresponding phase shift (due to the short-range potential) is increasing in the resonance by about  $\pi$  radians [7,8,21]. In Fig. 4 we show the short-range phase shifts  $\tau_{l\sigma}$  which are defined by equation,

$$\tau_{l\sigma} = \delta_{l\sigma} - \eta_l, \quad (2)$$

where  $\delta_{l\sigma}$  is the total phase shift, and  $\eta_l$  is the Coulomb part,  $\eta_l = \arg \Gamma(l+1-i/p)$ ,  $p$  being the photoelectron momentum. According to Fig. 4, the phase shift  $\tau_{f\sigma}$  increases in the resonance by about  $\pi$  radians as expected.

The main contribution to the  $\pi$  channels is given by the  $p\pi$  partial wave [see Fig. 3(b)]. There is the Cooper minimum in the  $f\pi$  partial cross section (which was absent in the

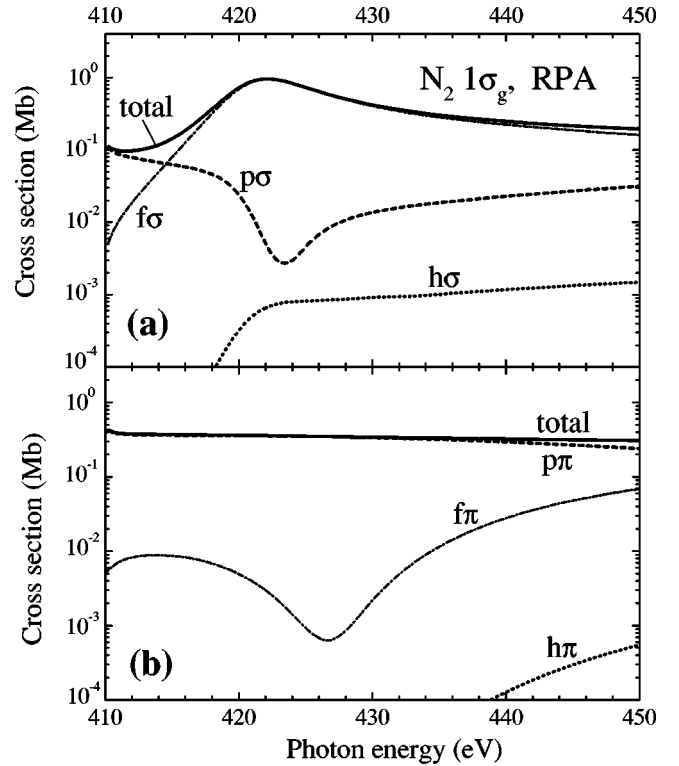


FIG. 3. (a) Partial photoionization cross sections corresponding to the transitions  $1\sigma_g \rightarrow \epsilon l\sigma_u$  with different values of orbital angular momentum  $l$  mentioned in the figure. (b) The same for the  $1\sigma_g \rightarrow \epsilon l\pi_u$  transitions.

RCHF approximation), but the contribution of this channel is anyway quite small at photon energies below 450 eV.

Figure 5 shows the RPA partial cross sections for the  $1\sigma_u$  shell. Here the main contribution near the resonance is given by the  $d\sigma$  partial wave. But though it shows seemingly a resonance behavior, the corresponding short-range phase shift shown in Fig. 4 is not increasing by  $\pi$  radians. Therefore one could not qualify it as a resonance, but rather as a correlational maximum due to the strong intershell interaction with the resonant  $1\sigma_g \rightarrow \epsilon\sigma_u$  channel.

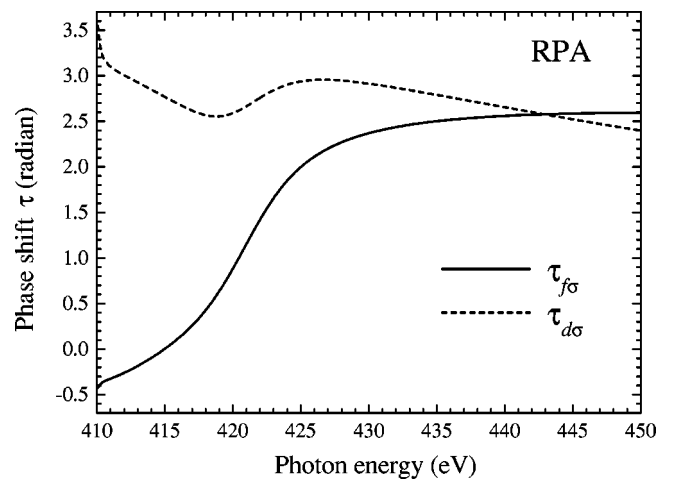


FIG. 4. Short-range phase shifts  $\tau_{l\sigma}$  for the  $1\sigma_g \rightarrow \epsilon f\sigma_u$  and  $1\sigma_u \rightarrow \epsilon d\sigma_g$  continuum channels in the RPA approximation.

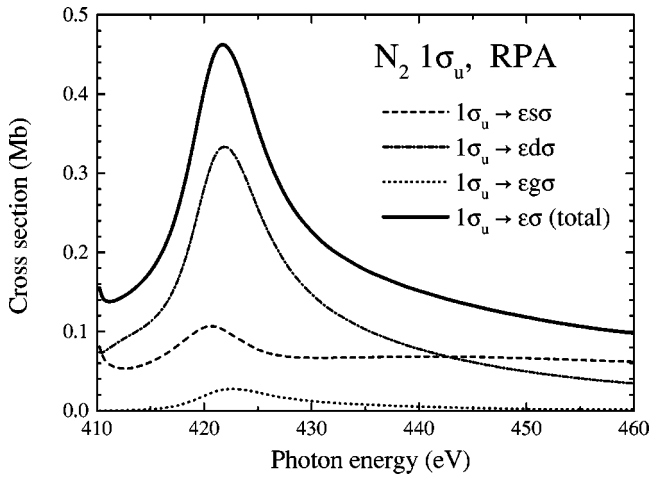


FIG. 5. Partial photoionization cross sections corresponding to the transitions  $1\sigma_u \rightarrow \epsilon l \sigma_g$  with different values of orbital angular momentum  $l$  mentioned in the figure.

The fact that the  $\sigma^*$  shape resonance reveals itself only in the  $\sigma$  transitions has been proved experimentally [22,23] by measuring the partial  $\sigma$  and  $\pi$  channel cross sections separately (denoted below as  $\sigma_\Sigma$  and  $\sigma_\Pi$ , respectively, with the  $\sigma_\Sigma$  being the sum of the  $1\sigma_g \rightarrow \epsilon\sigma_u$  and  $1\sigma_u \rightarrow \epsilon\sigma_g$  channels, and  $\sigma_\Pi$  being the sum of the  $1\sigma_g \rightarrow \epsilon\pi_u$  and  $1\sigma_u \rightarrow \epsilon\pi_g$  channels) using the angle-resolved photoion spectroscopy. Figure 6 shows the comparison between the RPA theory and experiment for the  $\sigma_\Sigma$  and  $\sigma_\Pi$  cross sections, as well as for their sum. The experimental data for the sum  $\sigma_\Sigma + \sigma_\Pi$  are normalized at 440 eV to the absolute photoabsorption cross section of  $K$  shell measured by Kempgens *et al.* [24] and also shown in Fig. 6. In our RPA cross section  $\sigma_\Sigma$  the position of the  $\sigma^*$  shape resonance is shifted to higher energies by about 3 eV, and above the resonance the cross section is decreasing

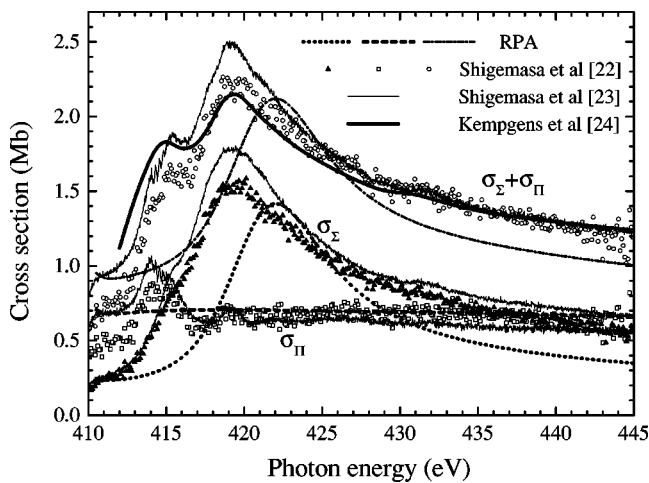


FIG. 6. Symmetry resolved cross sections  $\sigma_\Sigma$  and  $\sigma_\Pi$  and their sum calculated in RPA and measured in Refs. [22–24]. The absolute photoabsorption cross section of the  $K$  shell measured by Kempgens *et al.* in Ref. [24] is used for normalization (at 440-eV photon energy) of the relative cross sections measured in Refs. [22,23].

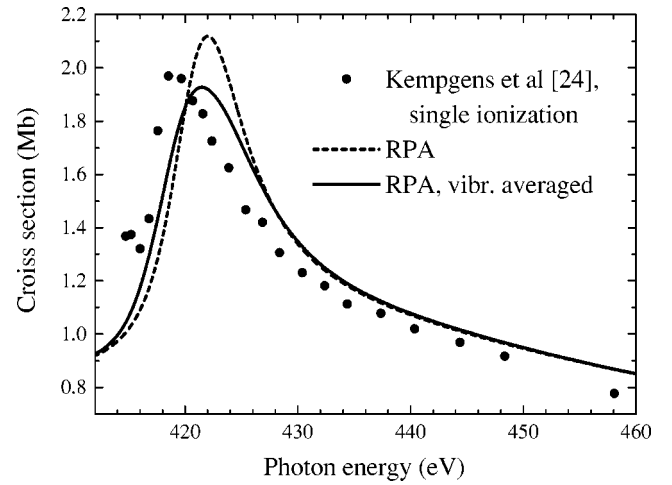


FIG. 7. Single electron photoionization cross section of the  $N_2$  molecule. Dashed line, RPA; solid line, RPA averaged over vibrational motion; dots, experimental cross section obtained by photoelectron spectroscopy [24].

too fast as compared to the experiment. The cross sections for the  $1\sigma_g \rightarrow \epsilon\pi_u$  and  $1\sigma_u \rightarrow \epsilon\pi_g$  channels in RPA are nearly equal at all photon energies considered in this paper and therefore are not shown separately. For their sum,  $\sigma_\Pi$ , the agreement with the experiment is rather good [the maximum at (413–416)-eV photon energy in the experiment is connected with the two-electron processes that are not included in the RPA]. Therefore for the total cross section the difference between the RPA and the experiment is essentially the same as for the  $\sigma_\Sigma$  cross section.

On the other hand, the photoabsorption cross section shown in Fig. 6, as well as the cross sections  $\sigma_\Sigma$  and  $\sigma_\Pi$  obtained by the angle-resolved photoion spectroscopy, include the contribution of two-electron processes, while the RPA cross section does not. Therefore it is more appropriate to compare our RPA results with the single electron photoionization cross section obtained by photoelectron spectroscopy in Ref. [24]. The corresponding comparison is made in Fig. 7. Now only the position of the shape resonance differ from the experiment, while above the resonance both the magnitude and the slope of the RPA cross section is in a good agreement with the experiment. In the same figure we show also the vibrational averaged cross section obtained by the integration over different internuclear distances according to Eq. (1). Though it does not differ much from the fixed-nuclei result, the shape resonance is slightly shifted to lower energies, which improves the agreement with the experiment.

Since the difference between the ionization thresholds of the  $1\sigma_g$  and  $1\sigma_u$  shells is small (about 0.1 eV), even smaller than the widths of the corresponding photoelectron lines, it seemed to be impossible to resolve these shells experimentally. Nevertheless, owing to essential increase of the experimental resolution, Hergenbahn *et al.* [25] succeeded to do it. Figure 8 shows the corresponding cross sections defined experimentally and calculated in both RCHF and RPA approximations, including the averaging of the RPA cross sections

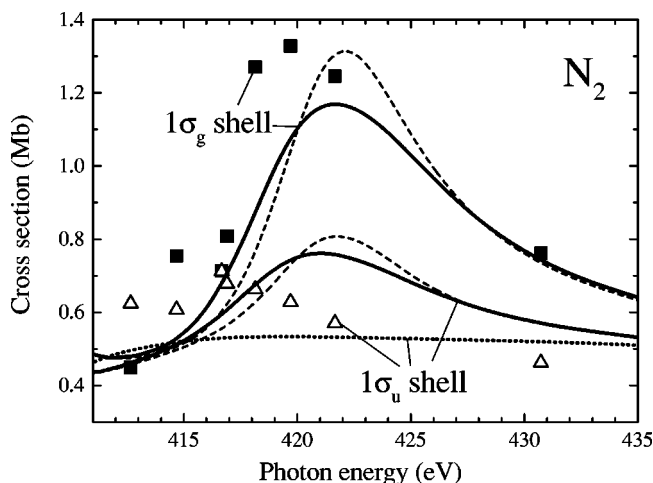


FIG. 8. Partial photoionization cross sections for  $1\sigma_g$  and  $1\sigma_u$  shells measured in Ref. [25] (squares and triangles), and calculated in RCHF approximation (dotted line), in RPA without vibrational averaging (dashed lines), and with vibrational averaging (solid lines).

over the internuclear distances. For the  $1\sigma_g$  shell, as before, the maximum in the RPA is shifted to higher energy compared to the experiment, while the shape of the cross section is well reproduced. For the  $1\sigma_u$  shell the experimental curve has also a maximum, while in the RCHF approximation, as well as in all other single-particle calculations, the cross section has no maximum in the region of the shape resonance. In the RPA approximation without vibrational averaging the maximum in the  $1\sigma_u$  cross section is higher than the experimental one, and shifted to higher energy. After the vibrational averaging the magnitude of the maximum is becoming lower and closer to the experimental one, while the position is still shifted to higher energy as a consequence of the analogous shift of the main maximum in the  $1\sigma_g$  shell. The positions of maxima in the  $1\sigma_g$  and  $1\sigma_u$  shells do not coincide in the experiment [25], while they coincide in the RPA. This difference can be connected with the part of correlations that is not included in the RPA. In recent calculation by Lin and Lucchese using multireference configuration interaction method [26] the corresponding maximum in the  $1\sigma_u$  cross section has the position close to the experimental one, but its magnitude is underestimated. As a result, we can conclude that the experiment [25] supports in general the existence of the correlational maximum predicted by theory [6], though a quantitative agreement between theory and experiment has not been reached.

#### IV. CONCLUSIONS

We have demonstrated that application of the RPA method for the photoionization of the  $K$  shell of the  $N_2$  molecule is as successful as it was for the valence shells in Ref. [1]. In general, the RPA results are in a good agreement with the

available experimental data. The main discrepancy is related with the shift of the maximum of the  $\sigma^*$  shape resonance in the RPA by about 3 eV to higher energies as compared to the experiment. In accord with the earlier prediction [7,8], from our calculations it follows that the  $\sigma^*$  shape resonance is formed by the contribution of practically one  $f\sigma_u$  partial wave. That takes place because accidentally at nearly the same photon energy there is a Cooper minimum in the  $p\sigma_u$  partial cross section, which was not mentioned previously. The results of our study show that unlike the atomic nitrogen [27], the many-electron correlations in the  $K$  shell of molecular nitrogen play an important role. Namely, it was demonstrated that due to the many-electron correlations between the  $1\sigma_u$  and  $1\sigma_g$  shells the correlational maximum appears in the nonresonant  $1\sigma_u$  shell at the photon energy of the  $\sigma^*$  shape resonance. This fact has been verified indirectly in Ref. [6]. The similar maximum was recently found also in the direct measurements of the corresponding partial cross sections [25], though the position of the experimental maximum for the  $1\sigma_u$  shell is shifted to lower photon energy compared to the  $\sigma^*$  shape resonance. The calculations have been performed both at a fixed equilibrium internuclear distance, and with the averaging over different internuclear distances to account for the vibrational motion in the ground state. This averaging, though not leading to strong changes, is improving the agreement with the experiment.

The present work, together with our recent investigation of the photoionization of  $H_2$  [5] and the valence shells of  $N_2$  molecule [1] demonstrates a high reliability of the RPA method for molecules. The method is capable to describe different kinds of experimental data available at the moment. In particular, it can describe the angular distributions of photoelectrons ejected from fixed-in-space molecules as it was recently demonstrated in [20,28], and can be used for obtaining a rather realistic predictions for all measurable quantities of photoionization process.

Though the results obtained here are rather encouraging, there are also some problems that need further consideration. In particular, the wrong position of the  $\sigma^*$  shape resonance in the RPA means that additional study of many-electron correlations need to be undertaken. Also, it is not possible to consider the two-electron processes within the RPA method, while they are important in some cases. Corresponding generalizations are possible, for example, by using the many-body perturbation technique.

#### ACKNOWLEDGMENTS

The authors are grateful to Dr. E. Shigemasa for sending the experimental results prior to publication, and to Dr. U. Hergenhan for sending his data in numerical form. The authors gratefully acknowledge the financial support of INTAS- RFBR Grant No. IR-97-471. N.A.C. also acknowledges the support of the Ministry of Education, Science and Culture of Japan extended to him at the last stage of this work, and is thankful to Professor A. Yagishita for helpful discussions.

- [1] S.K. Semenov, N.A. Cherepkov, G.H. Fecher, and G. Schönhense, *Phys. Rev. A* **61**, 032704 (2000).
- [2] I. Cacelli, R. Moccia, and A. Rizzo, *Phys. Rev. A* **57**, 1895 (1998).
- [3] L. Veseth, *J. Phys. B* **27**, 481 (1994).
- [4] R.R. Lucchese and R.W. Zuraes, *Phys. Rev. A* **44**, 291 (1991).
- [5] S.K. Semenov and N.A. Cherepkov, *Chem. Phys. Lett.* **291**, 375 (1998).
- [6] N.A. Cherepkov, S.K. Semenov, Y. Hikosaka, K. Ito, S. Motoki, and A. Yagishita, *Phys. Rev. Lett.* **84**, 250 (2000).
- [7] J.L. Dehmer and D. Dill, *Phys. Rev. Lett.* **35**, 213 (1975).
- [8] J.L. Dehmer and D. Dill, *J. Chem. Phys.* **65**, 5327 (1976).
- [9] T.N. Rescigno and P.W. Langhoff, *Chem. Phys. Lett.* **51**, 65 (1977).
- [10] D.L. Lynch and V. McKoy, *Phys. Rev. A* **30**, 1561 (1984).
- [11] I. Wilhelmy and N. Rosch, *Chem. Phys.* **185**, 317 (1994).
- [12] P. Lin and R.R. Lucchese, *J. Synchrotron Radiat.* **8**, 150 (2001).
- [13] J.L. Dehmer, D. Dill, and S. Wallace, *Phys. Rev. Lett.* **43**, 1005 (1979).
- [14] G. Raseev, H. Le Rouzo, and H. Lefebvre-Brion, *J. Chem. Phys.* **72**, 5701 (1980).
- [15] M.Ya. Amusia and N.A. Cherepkov, *Case Stud. At. Phys.* **5**, 47 (1975).
- [16] E.A. McCullough, Jr., *J. Chem. Phys.* **62**, 3991 (1977).
- [17] L. Laaksonen, P. Pyykkö, and D. Sundholm, *Comput. Phys. Rep.* **4**, 313 (1986).
- [18] Q. Zheng, A.K. Edwards, R.M. Wood, and M.A. Mangan, *Phys. Rev. A* **52**, 3945 (1995).
- [19] M.Ya. Amusia, V.K. Ivanov, S.A. Sheinerman, and S.I. Sheftel, *Zh. Eksp. Teor. Fiz.* **78**, 910 (1980) [*Sov. Phys. JETP* **51**, 458 (1980)].
- [20] S. Motoki, J. Adachi, K. Ito, K. Ishii, K. Soejima, A. Yagishita, S.K. Semenov, and N.A. Cherepkov, *Phys. Rev. Lett.* **88**, 063003 (2002).
- [21] R. G. Newton, *The Scattering Theory of Waves and Particles* (McGraw-Hill, New York, 1966).
- [22] E. Shigemasa, K. Ueda, Y. Sato, T. Sasaki, and A. Yagishita, *Phys. Rev. A* **45**, 2915 (1992).
- [23] E. Shigemasa, T. Gejo, M. Nagasono, T. Hatsui, and N. Kosugi, *Phys. Rev. Lett.* (to be published).
- [24] B. Kempgens, A. Kivimaki, M. Neeb, H.M. Koppe, A.M. Bradshaw, and J. Feldhaus, *J. Phys. B* **29**, 5389 (1996).
- [25] U. Hergenhahn, O. Kugeler, A. Rudel, E.E. Rennie, and A.M. Bradshaw, *J. Phys. Chem. A* **105**, 5704 (2001).
- [26] P. Lin and R.R. Lucchese, *J. Synchrotron Radiat.* **8**, 150 (2001).
- [27] N.A. Cherepkov, L.V. Chernysheva, V. Radojevic, and I. Pavlin, *Can. J. Phys.* **52**, 349 (1974).
- [28] T. Jahnke *et al.*, *Phys. Rev. Lett.* **88**, 073002 (2002).